THE JOURNAL OF BIOLOGICAL CHEMISTRY VOL. 291, NO. 5, pp. 2435–2443, January 29, 2016

Characterization of Tiki, a New Family of Wnt-specific Metalloproteases*

Received for publication, July 9, 2015, and in revised form, November 22, 2015 Published, JBC Papers in Press, December 2, 2015, DOI 10.1074/jbc.M115.677807

Xinjun Zhang[‡1], Bryan T. MacDonald[‡1], Huilan Gao[§], Michael Shamashkin[§], Anthony J. Coyle[§], Robert V. Martinez[§], and Xi He[‡2]

From the [‡]F. M. Kirby Neurobiology Center, Boston Children's Hospital, Department of Neurology, Harvard Medical School, Boston, Massachusetts 02115 and the [§]Centers for Therapeutic Innovation, Pfizer, Boston, Massachusetts 02115

The Wnt family of secreted glycolipoproteins plays pivotal roles in development and human diseases. Tiki family proteins were identified as novel Wnt inhibitors that act by cleaving the Wnt amino-terminal region to inactivate specific Wnt ligands. Tiki represents a new metalloprotease family that is dependent on Mn^{2+}/Co^{2+} but lacks known metalloprotease motifs. The Tiki extracellular domain shares homology with bacterial TraB/PrgY proteins, known for their roles in the inhibition of mating pheromones. The TIKI/TraB fold is predicted to be distantly related to structures of additional bacterial proteins and may use a core β-sheet within an α+β-fold to coordinate conserved residues for catalysis. In this study, using assays for Wnt3a cleavage and signaling inhibition, we performed mutagenesis analyses of human TIKI2 to examine the structural prediction and identify the active site residues. We also established an *in vitro* assay for TIKI2 protease activity using FRET peptide substrates derived from the cleavage motifs of Wnt3a and *Xenopus* wnt8 (Xwnt8). We further identified two pairs of potential disulfide bonds that reside outside the β-sheet catalytic core but likely assist the folding of the TIKI domain. Finally, we systematically analyzed TIKI2 cleavage of the 19 human WNT proteins, of which we identified 10 as potential TIKI2 substrates, revealing the hydrophobic nature of Tiki cleavage sites. Our study provides insights into the Tiki family of proteases and its Wnt substrates.

Wnt signaling plays pivotal roles in embryogenesis, homeostasis, and regeneration, and its dysregulation is implicated in many human diseases, notably cancer and metabolic disorders (1–4). The human genome contains 19 *WNT* genes that encode cysteine-rich ligands with a unique lipidation-palmitoleoylation, essential for their biogenesis and engagement with the Frizzled receptors (4). Wnt ligands appear to exhibit poorly defined specificity for Frizzled and several different Wnt co-receptors (LRP5/6, ROR1/2, RYK, and PTK7), which in combinations largely dictate the recruitment of intracellular proteins and downstream Wnt signaling outputs (5, 6). Wnt signaling is tightly regulated by various Wnt inhibitors (7). Most Wnt inhibitors, such as sFRP, DKK, WIF and SOST, antagonize Wnt signaling by binding to Wnt ligand or receptors and preventing Wnt-receptor interactions (7). We have recently identified a novel family of Wnt inhibitors, Tiki, named after the large-headed Polynesian statues and in reference to the Tiki overexpression phenotype in the frog (8). Our study suggested that Tiki proteins act as membrane bound proteases to cleave the amino-terminal region of Wnt proteins, thereby inactivating them. Tiki and another hydrolytic enzyme, Notum, which acts to remove a lipid modification of Wnt proteins (9, 10), represent a new mode of Wnt antagonism by modifications and inactivation of Wnt proteins.

Tiki is a metalloprotease that is inhibited by divalent metal chelators (EDTA or 1,10-phenanthroline) and shows a dependence on Mn^{2+} or Co^{2+}, whereas Ni^{2+}, Cu^{2+}, or Zn^{2+} does not promote enzymatic activity (8). Tiki cleavage sites for mouse Wnt3a (major, $SL_8 \downarrow AV$; and minor, $YS_{15} \downarrow SL$ or $SS_{16} \downarrow LG$; the number indicates the residue position in the mature Wnt3a protein) and Xwnt8 ($LT_{17} \downarrow YS$ and $SA_{19} \downarrow SV$) were determined by mass spectrometry and amino-terminal sequencing, revealing a relatively degenerate (although possibly hydrophobic) sequence requirement without a clear consensus for the Tiki protease. Thus, Tiki is able to remove the first 8, 15, or 16 amino acids from Wnt3a and the first 17 or 19 amino acids from Xwnt8 (8). The 19 human WNT proteins share little sequence identity in the amino terminus prior to the first common conserved cysteine (11), confounding the definition of a consensus Tiki proteolytic cleavage site. Tiki is probably an endopeptidase given that the inclusion of an amino-terminal HA epitope tag in HA-Wnt3a does not interfere with Tiki specificity or cleavage position (8). We also observed Tiki-mediated amino-terminal cleavage of mouse Wnt5a but not Xwnt11, suggesting Tiki specificity toward Wnt proteins (8).

Most vertebrates contain two *Tiki* genes (*TIKI1* and *TIKI2* in human) with a single, clearly identifiable homologue in primitive metazoans, including the *Nematostella* sea anemone and the *Amphimedon* sponge. The core 330-amino acid TIKI domain is around 25% identical with the uncharacterized GumN proteins from Gram-negative bacteria (Pfam protein family PF07446). Subsequently Pfam GumN merged into the TraB family (Pfam PF01963), joined chiefly by the presence of two conserved G*XX*H motifs. In Gram-positive bacteria, the plasmid encoded *TraB* gene functions to antagonize mating pheromone-induced conjugation and self-induction (12). PrgY

* The authors declare that they have no conflicts of interest with the contents of this article. The content is solely the responsibility of the authors and does not necessarily represent the official views of the National Institutes of Health.

[1] Both of these authors contributed equally to this work.

[2] An American Cancer Society Research Professor. Supported by National Institutes of Health Grants RO1-GM057603 and RO1-AR060359, by Grant MLSC 80253-01 from the Massachusetts Life Science Center, and by Boston Children's Hospital Intellectual and Developmental Disabilities Research Center (funded by National Institutes of Health Grant P30 HD-18655). To whom correspondence should be addressed. Tel.: 617-919-2257; Fax: 617-919-2771; E-mail: xi.he@childrens.harvard.edu.

from *Enterococcus faecalis* is the best studied TraB homologue (12–14). Based on their kinship with Tiki, we proposed that TraB/PrgY proteins inactivate mating pheromones composed of short hydrophobic peptides via proteolytic cleavage (15).

Tiki and TraB/PrgY proteins share limited sequence identity, but their predicted secondary structures reveal a similar placement of β-strands and α-helices to anchor several potential conserved catalytic residues (15), consistent with a common evolutionary origin. To gain insights into the novel TIKI/TraB/PrgY enzymatic domain, previously we used a sensitive fold recognition and structure prediction approach to build a three-dimensional template for the TIKI domain based on distantly related proteins with known crystal structures (15). Using these techniques, we and others constructed a model for the TIKI fold modeling on structures of bacterial proteins from the EreA/ChaN-like superfamily (15, 16). Six β-strands (βA–βF) in parallel/anti-parallel orientation formed the β-sheet core of our predicted TIKI $\alpha+\beta$-fold, aided by four key α-helices (α1, α6, α11, and α12), to bring together the conserved potential catalytic residues, including the two G*XX*H motifs, to one side of the three-dimensional model. The remaining eight predicted α-helices, contributing to nearly half of the TIKI domain and containing several conserved cysteine residues, do not directly contribute to the putative "catalytic surface" but may have roles in the integrity of the TIKI fold or specialized functions for each of the Tiki/TraB/PrgY proteins (15). These analyses provide informative clues for further characterizing the Tiki family of metalloproteases.

In the current study, we used mutagenesis approaches to characterize Tiki enzymatic activity and specificity. We also established an *in vitro* assay to monitor Tiki proteolytic function using FRET peptide substrates. Finally, we analyzed Tiki specificity toward all 19 human Wnt proteins.

Experimental Procedures

Plasmids—HA-Wnt3a, TIKI2N-FLAG-His (TIKI2 extracellular domain (amino acid residues 1–494) fused with a FLAG tag and a His_6 tag), and KRM2N-FLAG-His (Kremen2 extracellular domain (amino acid residues 1–363) fused with a FLAG tag and a His_6 tag) expressing constructs were described previously (8). TIKI2N mutants were generated via a PCR-based site-directed mutagenesis method using a TIKI2N-FLAG-His construct as the template. The HA- and V5-tagged human WNTs (HA-WNT-V5) were generated by introducing a HA tag after the predicted signal peptide of each WNT that already had a carboxyl-terminal V5 tag in the pcDNA3.2/V5-DEST vector (11).

Cell Culture, Transfection, and Dual-Luciferase Assay—HEK293T (ATCC, CRL-11268) cells were maintained in DMEM supplemented with 10% FBS and 1% penicillin-streptomycin-glutamine. Lipofectamine 2000 (Invitrogen) was used for all transfections. A SuperTopFlash reporter assay was performed as described previously (8).

Immunoblotting and Antibodies—Immunoblotting were performed as described previously (8). The following commercially available antibodies were used according to the manufacturer's instructions: anti-HA (catalog No. 3724, Cell Signaling, 1:1000), anti-FLAG (catalog No. 8146, Cell Signaling, 1:1000), anti-Wnt3a (catalog No. 2721, Cell Signaling, 1:1000), and anti-V5 (catalog no. V8012, Sigma, 1:2500).

Protein Purification and FRET Assay—Secreted KRM2N, TIKI2N, and TIKI2N mutants were purified from the conditioned medium of transfected HEK293T cells following the protocol described elsewhere (8). Wnt3a and Xwnt8 FRET peptides were synthesized by Cambridge Research Biochemicals, Ltd. The control peptide, 520 MMP FRET substrate II, was from Anaspec Inc. (catalog No. 60569-01). For the FRET assay, purified TIKI2N or KRM2N (a series of concentrations or 1 μg/ml) from the conditioned medium was incubated with FRET peptide (100 ng/ml final concentration) in PBS (50 μl) for 2 h at room temperature. The fluorescent signals (excitation 488 or 520 nm) were measured by a 96-well plate reader.

TIKI2 Enzyme Kinetics Measurement—A series of concentrations (in 1:2 serial dilutions with a starting concentration of 165 nM) of Wnt3a FRET peptide was incubated with excessive amount of TIKI2N (700 nM) in 50 μl of PBS for 2 h at 37 °C, and the fluorescent signals were measured. A standard curve for fluorescent signals (the blank background was subtracted) *versus* Wnt3a FRET peptide concentrations was plotted. For the enzyme kinetics assay, a series of concentrations of Wnt3a FRET peptide (in 1:2 serial dilutions with a start concentration of 1.65 μM) was incubated with TIKI2N (138 nM) or control buffer (serving as negative controls for background measurements) in 50 μl of PBS for 30 min at 37 °C, and the fluorescent signals were measured. The net fluorescent signal (the background signal was subtracted) for each substrate concentration was used in the standard curve to calculate the amount of FRET peptide cleaved by TIKI2N. The velocity (nM/min) at each substrate concentration was calculated. The velocity *versus* substrate concentration curve was plotted, and K_m, K_{cat}, and K_{cat}/K_m values were calculated using Prism 6 (GraphPad Software, Inc., San Diego) and a Michaelis-Menten model.

Results

Characterization of Tiki Enzymatic Active Site—Our previous results suggest that Tiki is a Mn^{2+}- or Co^{2+}-dependent metalloprotease (8). However, the sequence and predicted structure of the Tiki protein do not match any of the previously known metalloproteases (8). Our early interrogation of the potential Tiki active site focused on the two G*XX*H motifs, which were universally conserved in all Tiki and bacterial GumN proteins. G*XX*H motifs were initially classified as an extension of the Zinc-dependent H*EXX*H motif found in metzincin enzymes (H*EXXHXX*G*XX*H) (17). As Tiki proteins lack H*EXX*H motifs and are not zinc-dependent metalloproteases, the G*XX*H motifs of Tiki are distinct in context and function. Using the secreted form of the TIKI2 extracellular domain (TIKI2N-FLAG), which is necessary and sufficient for the Tiki protease function, we first mutated the histidines (His-58 and His-331) to alanines in the G*XX*H motifs plus an additional histidine, His-254, that is conserved down to nematodes (but not to bacteria) (Fig. 1*A*). We tested the TIKI2N enzymatic function by coexpression with an expression vector for HA-Wnt3a, which contains an amino-terminal HA and is active for Wnt signaling and suitable for Tiki-mediated cleavage as we demonstrated previously (8). TIKI2N cleaved the amino-terminal region of HA-Wnt3a as indicated by the HA

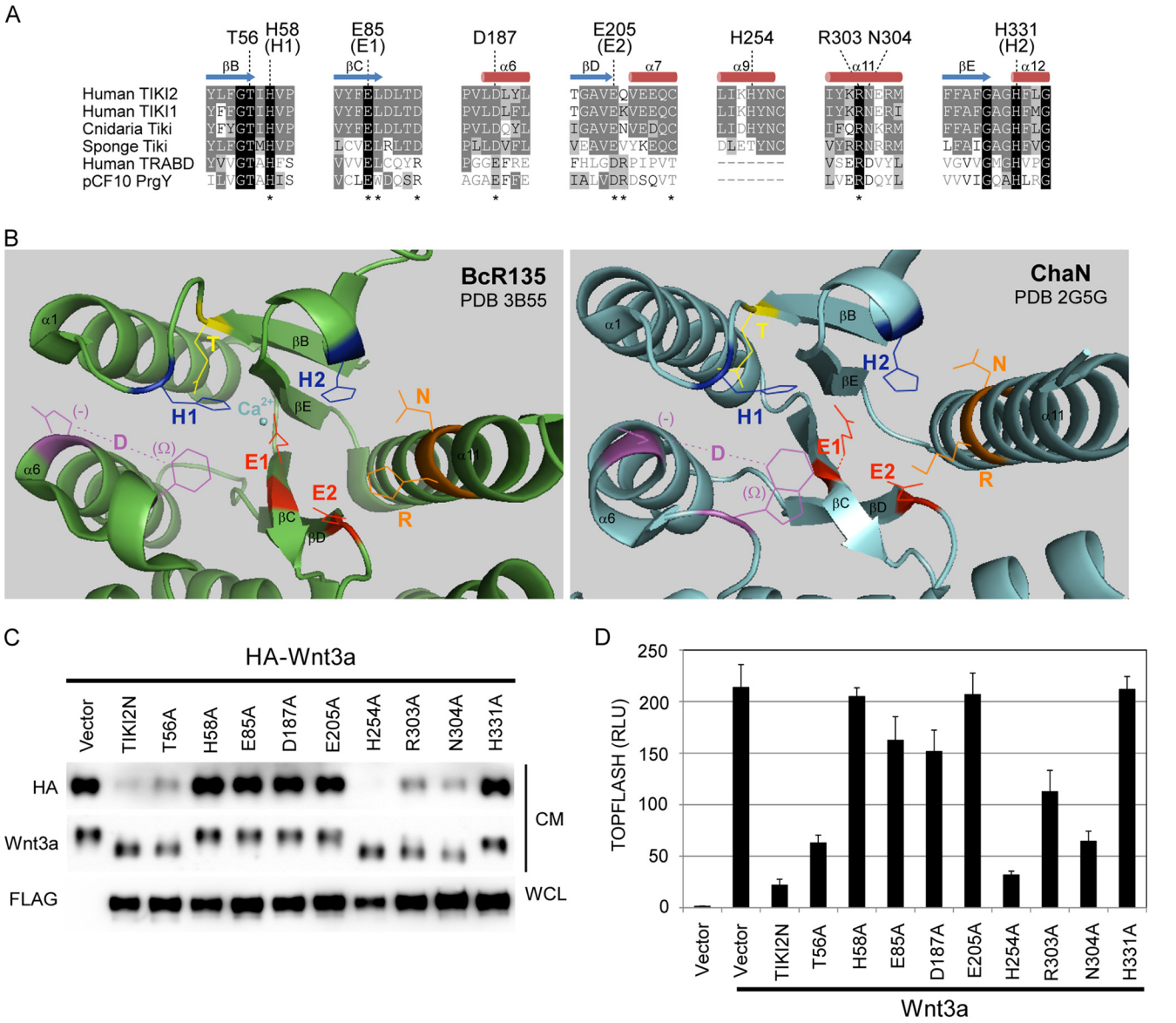

FIGURE 1. **Characterization of Tiki enzymatic active sites.** *A*, sequence alignment of TIKI/TraB domains from selected Tiki proteins, human TRABD, and bacterial PrgY. Predicted secondary structures and potential enzymatic active sites are shown. *Numbers* correspond to the residue positions in human TIKI2. *, indicates residues required for PrgY function (13). *B*, representative Tiki active site mapped onto the crystal structures of EreA-like BcR135 (PDB code 3B55) and ChaN (PDB code 2G5G). schematic model of BcR135 (*green*, residues 76–315) and ChaN (*cyan*, residues 39–150 and 182–224) with corresponding TIKI2 residues analyzed in this study *highlighted* and showing the side chains: T, *yellow* (BcR135 Glu-82 and ChaN Glu-46); H1, *blue* (BcR135 His-85 and ChaN His-48); E1, *red* (BcR135 Glu-113 and ChaN Glu-80); D, *magenta* (aromatic/acidic BcR135 Phe-141/Glu-145 and ChaN Trp-115/Asp-119); E2, *red* (BcR135 Asp-172 and ChaN Asn-138); R, *orange* (BcR135 His-283 and ChaN Arg-197); N, *orange* (BcR135 Asp-284 and ChaN Asp-198); and H2, *blue* (BcR135 His-309 and ChaN His-220). A lone Calcium metal from the BcR135 structure (PDB 3B55) is shown as a cyan dot in the presumptive active site. *C*, HA-Wnt3a and TIKI2N or TIKI2N mutants were coexpressed in HEK293T cells and conditioned medium (*CM*) or whole cell lysates (*WCL*) were analyzed by Western blotting with indicated antibodies. *D*, the activity of TIKI2N mutants in inhibiting Wnt3a induced SuperTopFlash reporter expression. Wnt3a and TIKI2N or TIKI2N mutants were coexpressed in HEK293T cells. Error bars represent S.D. in triplicates.

removal and the faster mobility of the remaining Wnt3a protein detected by an anti-Wnt3a antibody (Fig. 1*C*). TIKI2N H58A and H331A mutants were not able to either remove the HA tag or change the Wnt3a mobility; by contrast TIKI2N H254A was able to cleave the HA tag and increase the mobility similar to TIKI2N (Fig. 1*C*). Therefore each of the histidines of the two G*XX*H motifs is essential for the protease activity, but His-254 is not (and thus serves as a control for other experiments). We further analyzed TIKI2N-mediated inactivation of Wnt signaling using the SuperTopFlash Wnt reporter. Compared with the high activation levels from Wnt3a alone, coexpression of Wnt3a and TIKI2N resulted in a dramatic reduction of Wnt signaling (Fig. 1*D*). Consistent with HA-Wnt3a cleavage results, TIKI2N H58A and H331A mutants were unable to inhibit Wnt signaling, whereas the H254A mutant inhibited Wnt3a in a manner similar to TIKI2N (Fig. 1*D*). As a result of our functional characterization, we refer to His-58 and His-331 as the H1 and H2[3] positions, respectively, in the context of the TIKI domain (Fig. 1, *A* and *B*).

[3] The abbreviations used are: H1 and H2, His-58 and His-331, respectively; E1 and E2, Glu-85 and Glu-205, respectively; R, Arg-303; N, Asn-304; D, Asp-187; T, Thr-56; PDB, Protein Data Bank; MMP, matrix metalloprotease; FRET, fluorescence resonance energy transfer.

Using structure-guided searches for distant homologies to the TIKI domain, we and others have identified bacterial $\alpha+\beta$-fold protein structures from the EreA/ChaN-like superfamily: EreA-like *Bacillus cereus* proteins BcR135 and BcR136 (erythromycin esterase, Pfam PF05139, PDB codes 3B55 and 2QGM), ChaN (*Campylobacter* heme acquisition iron transporter, Pfam PF04187, PDB code 2G5G) and the C2 domain of PMT (*Pasteurella multocida* toxin, PDB code 2EBF) (15, 16). Importantly, a single metal ligand (likely Ca^{2+}) was observed between the histidine residues analogous to H1 and H2 in the BcR135 structure (PDB code 3B55, deposited by the Northeast Structural Genomics Consortium) (Fig. 1*B*). Based on our predicted TIKI domain model, the G*XX*H motifs are located at the edge of two β-strands (H1 after βB and H2 after βE), which are parallel and adjacent to each other within the β-sheet core (15). At least four other residues (Glu-85 (E1), Glu-205 (E2), Arg (R), and Asn (N)) (Fig. 1*A*) converge with the H1 and H2 residues in our predicted model, as shown in the context of the analogous active site residues in the BcR135 and ChaN structures (Fig. 1*B*). Two conserved glutamate residues at the end of βC (Glu-85 or E1) and βD (Glu-205 or E2) adopt a similar orientation to continue the β-sheet, with H1, H2, and E1 coordinating the metal ligand and E2 serving as catalytic residue to activate a water nucleophile (15). Tiki proteins also contain a highly conserved arginine-asparagine pair (Arg-303 and Asn-304 in TIKI2), analogous to known substrate stabilizing residues found in funnelin-type metalloproteases (17). Arg-303 and Asn-304 are located in a predicted extended α-helix that we juxtaposed between H2 and E2 in our model (15) (Fig. 1*B*). Therefore we generated additional mutants with alanine substitutions to test these potential metal-binding, catalytic, and substrate-stabilizing residues in our model: E1 (Glu-85), E2 (Glu-205), R (Arg-303), and N (Asn-304). A highly conserved threonine (Thr-56) preceding the H1 is present in Tiki/TraB proteins to form a consensus GT*X*H. This position, which is occupied by a glutamate residue in the distantly related bacterial proteins (GE*X*H in ChaN and PMT and GE*XX*H in EreA/BcR), appears to orient the H1 toward the metal-binding active site. The conserved TIKI2 Asp-187 within the predicted α-helix 6 is more difficult to model based on the existing structures. Alignments anchored by secondary structure point to acidic residues BcR135 Glu-145 and ChaN Asp-119 as possible analogous matches, although these residues are at the periphery of the presumptive active sites (Fig. 1*B*). Another candidate location for TIKI2 ASP-187 could be the aromatic residues BcR135 Tyr-141 and ChaN Trp-115, which orient toward the H1 and E1 residues (Fig. 1*B*). Therefore, at the moment it is unclear whether Asp-187 (D) contributes to the catalytic core or performs a role similar to TIKI2 Thr-56 in orienting the H1 and/or E1 residues. We note that in an alternate model of the Tiki active site, Asp-187 is shown in place of E2 (16). Given the importance of the H1 position, we also analyzed alanine mutations at the T (Thr-56) and D (Asp-D187) positions to examine whether they act as non-catalytic but active site stabilizing residues.

Similar to the TIKI2N H1 and H2 mutants, alanine mutations at E1, D, or E2 were unable to cleave HA-Wnt3a or change Wnt3a mobility (Fig. 1*C*). Mutations at the T, R, and N positions resulted in detection of residual HA-tagged Wnt3a, with a majority of the Wnt3a proteins exhibiting faster mobility (Fig. 1*C*). Therefore, mutations at the H1, E1, D, E2, or H2 position each abolished TIKI2 protease activity, whereas mutations at T, R, or N reduced but did not abolish it.

We next examined the ability of these additional TIKI2N mutants to inhibit Wnt3a signaling (Fig. 1*D*). Mutation at E2, like those at H1 and H2, completely abolished TIKI2-mediated inhibition of Wnt3a signaling in the SuperTopFlash reporter assay (Fig. 1*D*). Mutation of E1 or D significantly compromised TIKI2N function in Wnt3a inhibition, whereas mutation at R had a moderate effect (Fig. 1*D*). On the other hand, mutation at T or N only mildly affected TIKI2N function, permitting significant inhibition of Wnt3a when compared with TIKI2N WT or the control H254A mutant (Fig. 1*D*).

Thus these data on Wnt cleavage and functional inhibition by Tiki support our structural modeling of the conserved TIKI catalytic domain (15), and identify key residues for the Tiki protease activity. Given that metalloproteases often use His, Glu, and Asp residues as metal ligands and use one Glu as the catalytic residue (17, 18), these results are consistent with our earlier findings that Tiki family proteins are metalloproteases.

Monitoring Tiki Enzymatic Activity in Vitro Using FRET Peptide Substrates—To monitor Tiki activity *in vitro*, we designed a FRET peptide cleavage assay. We purified TIKI2N and mutant proteins from conditioned medium of transfected HEK293T cells using a FLAG tag-based affinity purification approach (8) (Fig. 2*A*). The Tiki cleavage sites in Wnt3a and Xwnt8 have been determined by mass spectrometry and Edman sequencing (8). We synthesized two peptides that cover the cleavage sites in Wnt3a (YPIWWS↓LAVGPQY) and Xwnt8 (AYLT↓YS↓ASVAVGAQ) and a Wnt3a mutant peptide (YPIWW**DD**AVGPQY, underlined aspartate substitutions) that has an altered cleavage site and does not permit Tiki cleavage of Wnt3a (8). Each of these peptides was conjugated with an amino-terminal QSY-7 succinimidyl ester (quencher) group and a carboxyl-terminal Alexa Fluor 488 (AF488, fluorophore) group (Fig. 2*B*). The recombinant TIKI2N protein and the FRET peptides were used in the *in vitro* reaction. TIKI2N cleaved Wnt3a and Xwnt8 peptides at an EC_{50} below 0.5 μg/ml, whereas KRM2N, which corresponds to the extracellular domain of human Kremen2 and was used as a negative control (19), was unable to cleave either Wnt3a or Xwnt8 peptide (Fig. 2, *C* and *D*). Neither TIKI2N nor KRM2N cleaved the Wnt3a mutant peptide (Fig. 2*C*). TIKI2N did not cleave a control FRET peptide that was a substrate for the metalloprotease MMP (Fig. 2*E*), further indicating Tiki enzymatic specificity in this *in vitro* assay. Next, we examined the TIKI2N mutants by using the Wnt3a FRET peptide (Fig. 2*F*). Consistent with the results using HA-Wnt3a as the substrate (Fig. 1*B*), TIKI2N and the H254A mutant cleaved the Wnt3a peptide with identical efficiency (Fig. 2*F*). Mutation at the H1, E1, D, E2, or H2 site resulted in complete loss of TIKI2 cleavage activity. The TIKI2N T mutant retained approximately half of the peptide cleavage activity. Somewhat surprisingly, the R mutant was almost completely inactive in the FRET peptide assay (Fig. 2*F*) whereas it had partial activity in HA-Wnt3a cleavage and

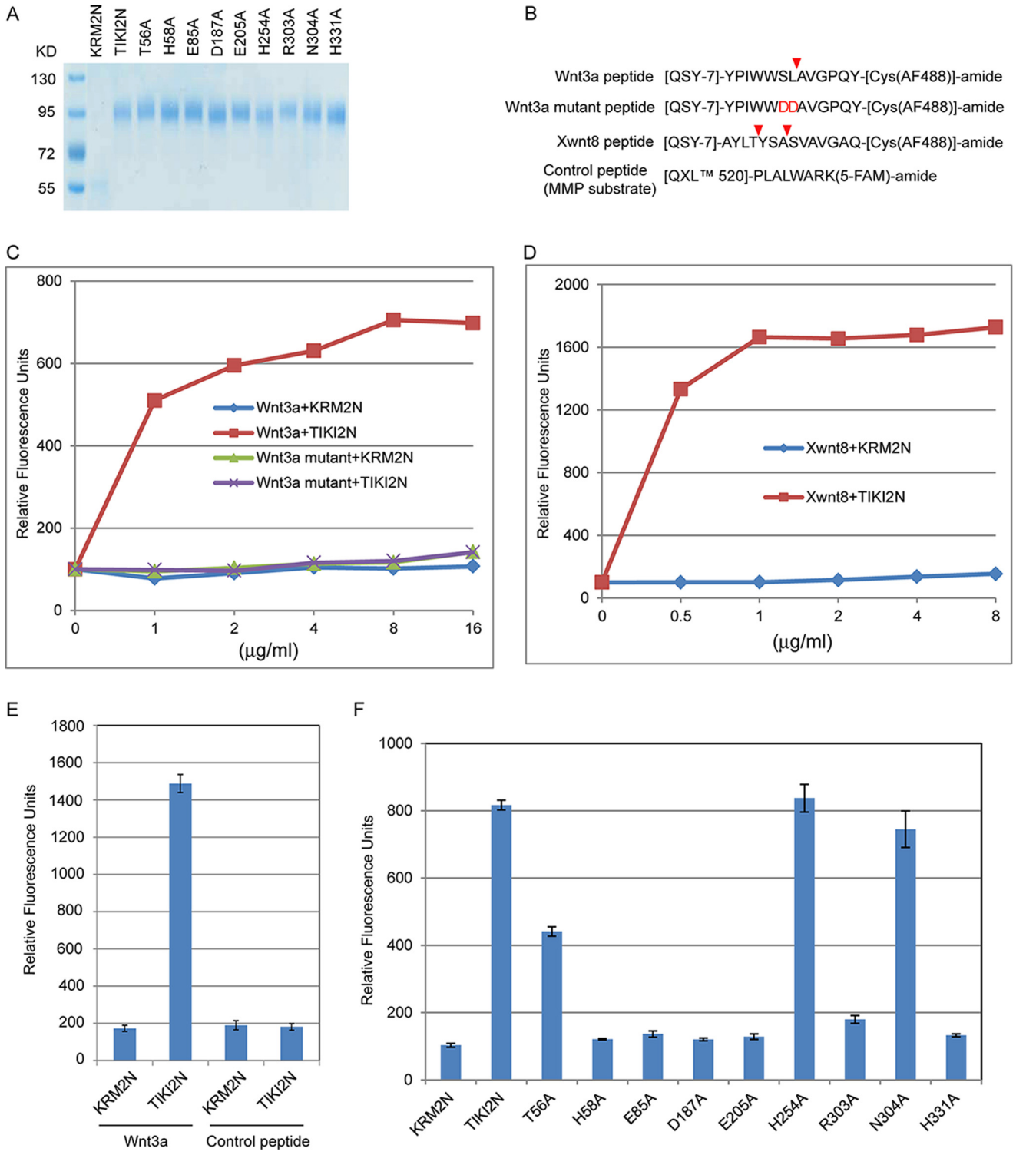

FIGURE 2. **Analysis of Tiki activity *in vitro* using FRET peptide substrates.** *A*, SimplyBlue staining of purified recombinant TIKI2N and KRM2N (negative control) proteins on SDS-PAGE. *B*, FRET peptide substrates corresponding to Wnt3a (YPIWWSLAVGPQY), Wnt3a mutant (YPIWW*DD*AVGPQY), Xwnt8 (AYLTYSASVAVGAQ), and a negative control (PLALWARK, a MMP substrate). In the Wnt3a mutant peptide the "SL" residues were changed to "DD." *Arrowheads* indicate Tiki cleavage sites. *C*, recombinant TIKI2N, but not KRM2N, cleaves the Wnt3a peptide but not the Wnt3a mutant peptide in a dose-dependent manner. *D*, TIKI2N but not KRM2N cleaves the Xwnt8 peptide in a dose-dependent manner. *E*, TIKI2N cleaves the Wnt3a peptide but not the negative control peptide. *F*, analysis of the activity of TIKI2N mutants in cleaving the Wnt3a peptide.

Wnt3a inhibition assays (Fig. 1, *C* and *D*). On the other hand, the neighboring N mutant was largely active in these three assays (Figs. 1, *C* and *D*, and 2*F*). Overall, the activity data assessed by the *in vitro* Wnt3a peptide assay correlated strongly with the results of HA-Wnt3a cleavage and functional Wnt inhibition.

To assess the enzymatic efficiency of TIKI2 in Wnt cleavage, we determined the enzyme kinetics parameters using the

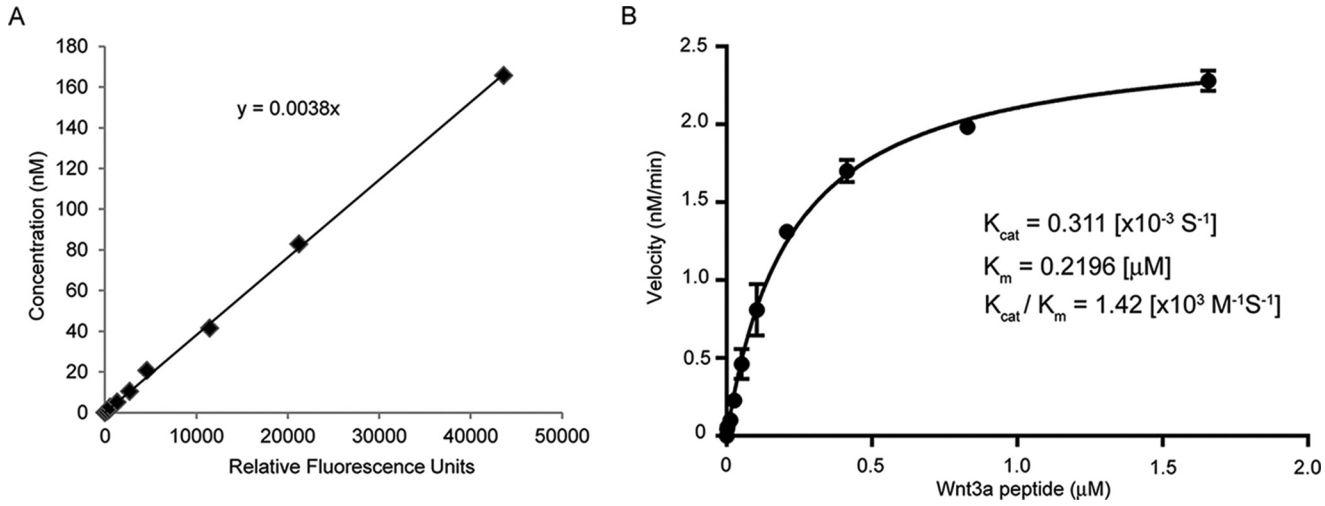

FIGURE 3. **TIKI2N enzyme kinetics assay.** *A*, standard curve for fluorescent signal *versus* cleaved Wnt3a FRET peptide. An excessive amount of TIKI2N was used to ensure the complete cleavage of Wnt3a FRET peptide. *B*, Michaelis-Menten plot of Wnt3a FRET peptide with 138 nM TIKI2N. K_{cat}, K_m, and K_{cat}/K_m values were calculated.

recombinant TIKI2N protein and the Wnt3a FRET peptide (Fig. 3). K_{cat} (0.311×10^{-3} s^{-1}), K_m (0.22 μM), and K_{cat}/K_m (1.42×10^3 $M^{-1}s^{-1}$) values of TIKI2 appear to be comparable with those of other metalloproteases (20). Taken together, these results support the characterization of Tiki proteins as Wnt-specific metalloproteases.

Analysis of Conserved Cysteines in TIKI Domain—Secreted proteins often contain disulfide bonds that are important for protein folding and stability. Sequence alignment indicates that TIKI domain contains four conserved cysteines, which in human TIKI2 are Cys-29 (c1), Cys-100 (c2), Cys-211 (c3), and Cys-257 (c4). The first conserved cysteine is in the unstructured amino terminus, and the other three follow helices α2, α7, and α9, respectively (Fig. 4*B*). The cysteine-containing regions within the TIKI domain could not be modeled using templates from the bacterial protein EreA-like, ChaN, or PMT structure. To assess the role of these cysteines in Tiki enzymatic activity and potential disulfide bond formation, we generated a series of single and double cysteine mutants and coexpressed each of them with Wnt3a in HEK293T cells (Fig. 4*A*). Human TIKI2 contains an additional extracellular cysteine (Cys-323) at the beginning of βE (on the opposite side from the second G*XX*H motif), although this is not conserved among Tiki proteins or even in the frog Tiki2. To test the importance of this non-conserved cysteine we mutated human TIKI2 to resemble frog Tiki2, IC322SF (c5), and used it together with a TIKI2N inactive mutant, H58A/H331A, as control. TIKI2N and the c5 mutant efficiently cleaved Wnt3a and resulted in significant Wnt3a band shifts on Wnt3a Western blot as compared with Wnt3a coexpressed with the H58A/H331A mutant (Fig. 4*A*). The activity of the four conserved cysteine mutants was reduced to different extents (Fig. 4*A*). Among the double mutants, c1-c2, c1-c3, c2-c4, and c3-c4 were largely inactive, whereas c1-c4 and c2-c3 were almost fully active (Fig. 4*A*). These results are consistent with the possibility that there are two disulfide bonds, one formed by c1-c4 and one by c2-c3 (Fig. 4*B*). This also appears to be consistent with our predicted TIKI domain-folding topology, with βC and βD strands in close proximity to accommodate a c2-c3 disulfide bond and intercalation of βE closer to the amino-terminal β-strands to allow a c1-c4 disulfide bond (15). Although the Tiki α-helical bundles (α2-α5 and α7-α10) share no similarity to the bacterial EreA/ChaN-like structures, ChaN contains analogous α-helical bundle insertions (Fig. 4*C*, *insert 1* in *green* and *insert 2* in *wheat*), which are spatially located above and around the presumed active site. Superimposing the locations of the Tiki cysteines on the ChaN structure illustrates the potential for these disulfide bond connections and provides further support for likely Tiki c1-c4 and c2-c3 disulfide bond organization (Fig. 4*C*). The two potential disulfide bonds may contribute to the stability of the TIKI domain structure or may assist in Wnt protein substrate recognition in the Tiki-specific α-helical regions.

Characterization of Tiki Specificity toward Wnt Proteins—We have shown that Tiki cleaves mouse Wnt3a, mouse Wnt5a, and Xwnt8 but not Xwnt11, suggesting that Tiki specifically cleaves some but not all Wnt proteins (8).

To further study Tiki specificity, we systematically examined TIKI2 cleavage of each of the 19 human WNT proteins. A HA tag and a V5 tag were fused to the amino and carboxyl termini, respectively, of each WNT, and each of these double-tagged WNT proteins was expressed in HEK293T cells alone or with TIKI2N. Whole cell extracts were analyzed by Western blotting with anti-HA and anti-V5 antibodies. WNT cleavage was assessed by the reduction of HA signal or by mobility shift of the V5 signal (Fig. 5*A*). The results indicate that TIKI2 cleaved WNT2B, -3, -3A, -4, -5A, -5B, -6, -8A, -8B, and -16 but not WNT1, -2, -7A, -7B, -9A, -9B, -10A, or -10B (Fig. 5*B*). Therefore TIKI2 appears to be able to cleave 10 of the 19 WNT proteins, and the cleavage occurs strictly at the WNT amino terminus.

Wnt proteins are conserved in amino acids throughout most of the molecules, but their amino-terminal sequences are variable among family members although conserved among paralogues (11). We noticed previously that the sequences flanking the Tiki cleavage sites in Wnt3a and Xwnt8 are very different (Fig. 2*B*) (8). Comparisons among Tiki-cleavable Wnt *versus*

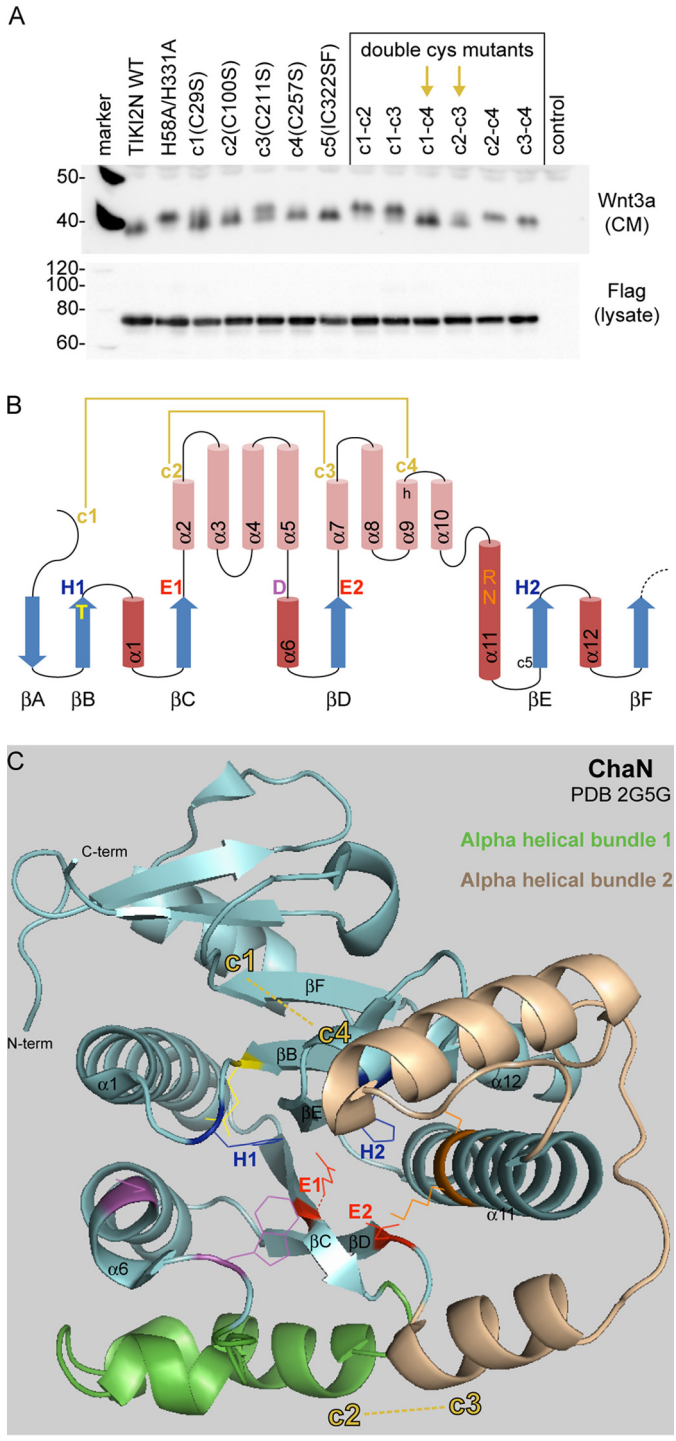

FIGURE 4. **Characterization of conserved cysteines in TIKI domain.** *A*, Wnt3a and TIKI2N or TIKI2N mutants were coexpressed in HEK293T cells, and the resulting conditioned medium (*CM*) and whole cell lysates were analyzed by Western blotting. The differential migration of Wnt3a indicates TIKI2N cleavage activity. Note that the H58A/H331A double mutant is functionally inactive as is each single mutant; the TIKI2-specific c5 (IC322SF) mutant is fully active; the single cysteine c1, c2, c3, and c4 mutants are partially active; and only the double cysteine c1-c4 and c2-c3 are active. *B*, predicted secondary structure of Tiki. β-Strands A–F make up the core β-sheet of the TIKI domain flanked by *darkly shaded* α-helices 1, 6, 11, and 12. *Lightly shaded* α-helices 2–5 and 7–10 within the TIKI domain are unplaced in the current simulated model for active sites. Located outside of the TIKI domain and omitted from the diagram are an additional predicted β-strand (βG) and α-helix (α13) of unassigned functions. Two potential disulfide bonds are indicated by *connecting lines*, and putative enzymatic active sites are also indicated. *C*, schematic model of ChaN (PDB code 2G5G, residues 9–263) with corresponding

non-cleavable Wnt did not appear to yield a consensus cleavage sequence but seemed to reinforce the notion that the amino termini of Tiki-cleavable Wnt are relatively hydrophobic, whereas the amino termini of non-cleavable Wnt often contain more charged and polar residues (11). Consistent with this notion, Tiki did not cleave FLAG-Wnt3a (the FLAG tag DYKDDDDK is at the amino terminus) (data not shown), the Wnt3a mutant that harbors four aspartate substitutions of the major and minor cleavage sites (SYPIWW**DD**AVGPQYS**DD**GS . . .) (8), or Wnt3a mutant peptide (YPIWW**DD**AVGPQY) (Fig. 2, *B* and *C*).

Indeed although WNT2 and WNT2B are closely related and their amino-terminal sequences are relatively conserved, TIKI2 cleaved WNT2B but not WNT2 (Fig. 5*A*). The amino-terminal sequence alignment of WNT2 and -2B indicates that two residues in WNT2, Arg-40 and Thr-42, make the WNT2 amino terminus more hydrophilic than that of WNT2B, in which the two corresponding residues are Gly and Leu, respectively (Fig. 5*C*). We hypothesized that these two residues might determine the Tiki cleavage specificity. We generated three mutants of WNT2, R40G, T42L, and R40G/T42L, in which one of these residues was changed to Gly and Leu, respectively, or both were changed to Gly and Leu together. We examined the TIKI2 cleavage of these WNT2 mutants by coexpressing each with TIKI2N. As shown in Fig. 5*D*, TIKI2N cleaved the WNT2 R40G/T42L mutant and also the WNT2 R40G mutant, albeit less effectively. These results suggest that the hydrophobicity of the Wnt amino terminus is a major determinant of Tiki cleavage susceptibility.

Discussion

Tiki proteins form a new family of Wnt antagonists and act as metalloproteases that cleaves the Wnt amino terminus (8). In this study, we analyzed potential enzymatic active sites of TIKI2 and characterized the Wnt substrate specificity of TIKI2. Our study establishes that the Tiki metalloprotease family has unique enzymatic characteristics, supporting its classification in MEROPS database as metallopeptidase family M96.

Tiki/TraB/PrgY family proteins do not harbor known metalloprotease motifs but contain two conserved *GXXH* motifs (8, 15). Two previous studies used bioinformatics approaches to model the enzymatic fold of the TIKI domain (15, 16). Both of those studies suggest that the TIKI domain is related to bacterial proteins from the EreA/ChaN-like superfamily, including the erythromycin esterase family members BcR135 and BcR136, the heme-binding ChaN iron transporter, and the uncharacterized C2 subdomain from PMT. Of these structures, a metal ligand was only found in the BcR135 presumptive active site (PDB code 3B55). No metal was present in the BcR136 structure (PDB code 2QGM), consistent with functional data showing that hydrolase activity has been observed for BcR136 and EreB but not EreA in the presence of chelators (21).

TIKI2 residues analyzed in this study are *highlighted* according to descriptions in the legend for Fig. 1. ChaN α-helical insert 1 (*green*, residues 84–113) and insert 2 (*wheat*, residues 140–182) are analogous to the Tiki α2-α5 and α7-α10 inserts, respectively. The relative positions of the Tiki c1-c4 and c2-c3 disulfide bond connections are overlaid on the ChaN structure.

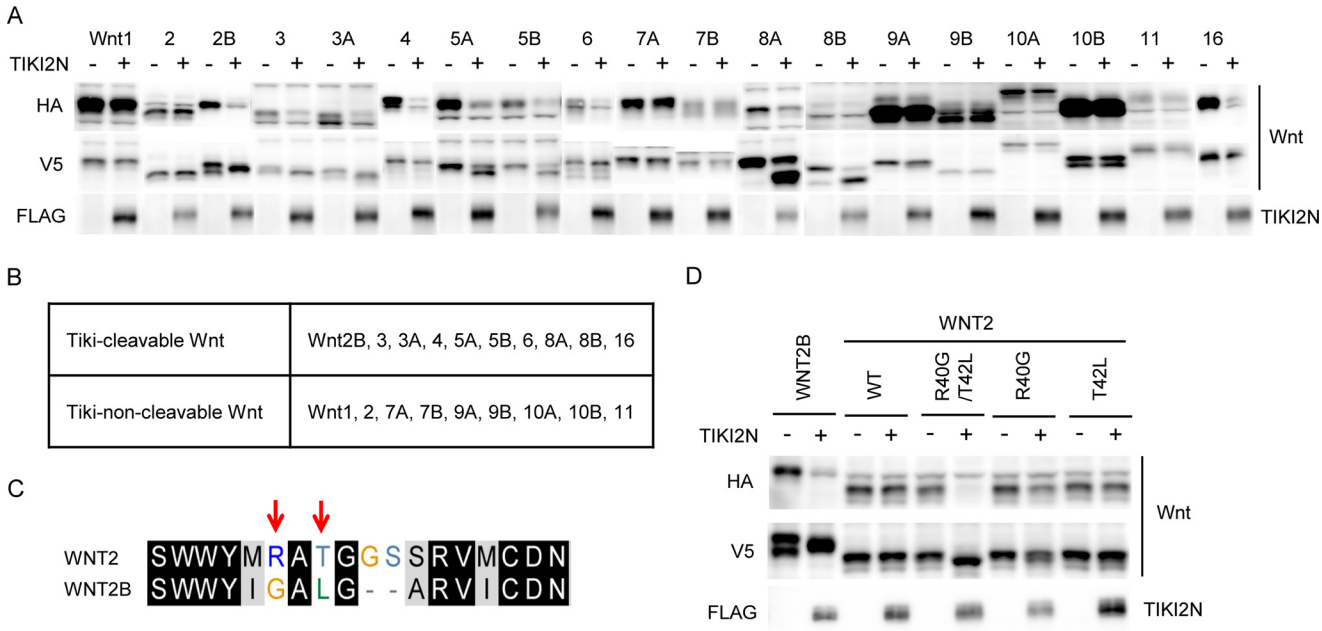

FIGURE 5. **The specificity of Tiki for 19 human WNT proteins.** *A*, each of the 19 human WNT with an HA and a V5 tag on each terminus was expressed alone or coexpressed with TIKI2N, and whole cell lysates were analyzed by Western blotting with the indicated antibodies. Reduction of the HA signal and a mobility shift of the V5 signal in the presence of TIKI2N expression indicate an amino-terminal cleavage of the WNT protein by TIKI2N. *B*, summary of Tiki-cleavable and non-cleavable WNT. *C*, sequence alignment of the amino terminus of WNT2 and WNT2B. *Arrows* indicate WNT2 (non-cleavable) Arg-40 and Thr-42 residues that were altered to corresponding WNT2B (cleavable) residues. *D*, WNT2B, WNT2, and WNT2 mutants were each expressed alone or with TIKI2N in HEK293T cells, and whole cell lysates were analyzed by Western blotting.

Although it is unclear whether EreB acts as a metalloprotease, EreB mutants for the corresponding active site positions H1 (H46A), E1 (E74A), and H2 (H288A) display loss of function in an erythromycin cleavage assay (21). Partial loss of function was also observed for EreB E43A mutant in the G*EXX*H motif, analogous to TIKI2 GT*X*H.

Based on the known structural information for this group of proteins, a TIKI domain topology was predicted in which the His residue in two G*XX*H motifs and conserved Glu, Asp, Arg, and Asn residues between the G*XX*H motifs are mapped to the putative enzymatic core. Although mutation at Thr-56 resulted in partial loss of function, this data effectively rules out Thr-56 as a candidate nucleophile. The results from the mutagenic analysis of TIKI2 suggest that both conserved His residues (H1 and H2) and the conserved Glu and Asp residues highlighted by the two predicted models (15, 16) (Fig. 1, E1, D, and E2) are required for TIKI2 activity (Figs. 1 and 2). The only disagreement between these two predictions is whether a second Glu (E2, Glu-205 in TIKI2) or an Asp (D, Asp-187 in TIKI2) residue is an active site (15, 16). Because we observed an equivalent loss of function for the D and E2 residues, our functional data do not favor one model over the other. However it does put in question how many metal ions are within the active site. These widely spaced residues in the TIKI domain may come together in the three-dimensional structure and coordinate one or two metal ions (Co^{2+} or Mn^{2+}) (8) to form the catalytic core. Although this pattern of the enzymatic active site in the TIKI domain is unique among metalloprotease families, there is precedence for co-catalytic Co^{2+}/Mn^{2+}-dependent metalloproteases (18). A crystal structure of the TIKI domain will be critical to further define the enzymatic activity of Tiki family metalloproteases.

Our *in vitro* data for the TIKI2 mutants using the Wnt3a FRET peptide are largely consistent with cleavage of HA-Wnt3a and functional inactivation of Wnt signaling. The only exception was for the Arg (R303A) mutant that was largely dead in the FRET assay but remained partially active in the other two assays. Although completely conserved in Tiki homologues, the Arg/Asn residues are variable compared with that of TraB/PrgY (RD), ChaN (KD), EreA (RD), EreB (KD), and BcR (HD). Notably, TIKI2 Asn-304 is unique, and the lack of conservation may support a role for substrate recognition or stabilization of the active site. These requirements may be less stringent for a short Wnt3a FRET peptide than for the full-length Wnt3a protein.

Bacterial TraB and PrgY are plasmid-encoded transmembrane proteins with extracellular TraB domains that are homologous to the TIKI domain (15). TraB/PrgY proteins function to reduce the amount of the autocrine pheromone by an unknown mechanism to prevent self-induction (12). Two possible models of TraB/PrgY function have been proposed: by binding the pheromone and delivering it to a cell wall protease for degradation or by acting as a protease and directly degrading bound pheromone (12). Our studies support the idea that TraB/PrgY proteins are metalloproteases that directly degrade bound pheromone. Consistent with this model, mutagenic analysis of PrgY has demonstrated that several conserved residues in the TraB domain are required for its function, including the H1, E1, D, E2, and R equivalents in TIKI2 (Fig. 1*A*) (13). Our study also suggests that the TraBD (TraB domain-containing) protein, which exists in most organisms in metazoan, may act as a metalloprotease. However, TraBD is unlikely to cleave Wnt pro-

teins, as it lacks a predicted signal peptide and likely functions as a cytoplasmic protein.

We reported previously that Tiki cleaves mouse Wnt3a, mouse Wnt5a, and Xwnt8 but not Xwnt11 (8). We have systematically analyzed TIKI2 cleavage of the 19 human WNT proteins. Based on the Tiki cleavage susceptibility, we have classified WNT proteins into Tiki-cleavable and non-cleavable groups. TIKI2 cleavage does not appear to follow a stringent consensus sequence, except that the sequences that flank cleavage sites are relatively hydrophobic. It is interesting to note that all known bacterial sex pheromones, which are putative TraB/PrgY substrates, are hydrophobic hepta- or octapeptides, such as LVTLVFV and LFSLVLAG (22). We also note that in addition to the 13-residue FRET Wnt3a peptide (YPIWWS-↓LAVGPQY), shorter FRET Wnt3a peptides, IWWS-↓LAVGP and WWS↓LAVG, also displayed similar TIKI2N cleavage (data not shown), suggesting that TIKI, like TraB/PrgY, is capable of cleaving short hydrophobic peptides analogous to bacterial pheromones. However, TIKI2 cleavage of the 10 cleavable WNT proteins is strictly at the amino terminus, as we noted previously (Fig. 5*A*) (8). We have shown that TIKI2 binds to mouse Wnt3a, Wnt5a, Xwnt8, and Xwnt11, but it cleaves Wnt3a, Wnt5a, and Xwnt8 but not Xwnt11 (8). These results taken together suggest two steps of Tiki cleavage of Wnt proteins: Tiki interacts with a conserved region within Wnt proteins, thereby possibly orienting the Wnt amino terminus for Tiki cleavage, which requires the hydrophobic nature of the cleavable amino terminus. Our results will guide future studies on the regulation of Wnt functions by the Tiki metalloprotease family.

Author Contributions—X. Z., B. T. M. and X. H. conceived and coordinated the study and wrote the paper. X. Z. and B. T. M. designed, performed, and analyzed most of the experiments. H. G. and R. V. M. helped design the FRET peptides and FRET assays. M. S. contributed to protein purification. A. J. C. and R. V. M. directed the research related to this study at Pfizer. All authors reviewed the results and approved the final version of the manuscript.

Acknowledgments—We thank members of the He laboratory and J. Fernando Bazan for helpful discussions and comments.

References

1. Anastas, J. N., and Moon, R. T. (2013) WNT signalling pathways as therapeutic targets in cancer. *Nat. Rev. Cancer* **13,** 11–26
2. Clevers, H., and Nusse, R. (2012) Wnt/β-catenin signaling and disease. *Cell* **149,** 1192–1205
3. MacDonald, B. T., Tamai, K., and He, X. (2009) Wnt/β-catenin signaling: components, mechanisms, and diseases. *Dev. Cell* **17,** 9–26
4. Willert, K., and Nusse, R. (2012) Wnt proteins. *Cold Spring Harb. Perspect. Biol.* **4,** a007864
5. van Amerongen, R. (2012) Alternative Wnt pathways and receptors. *Cold Spring Harb. Perspect. Biol.* **4,** a007914
6. MacDonald, B. T., and He, X. (2012) Frizzled and LRP5/6 receptors for Wnt/β-catenin signaling. *Cold Spring Harb. Perspect. Biol.* **4,** a007880
7. Cruciat, C. M., and Niehrs, C. (2013) Secreted and transmembrane wnt inhibitors and activators. *Cold Spring Harb. Perspect. Biol.* **5,** a015081
8. Zhang, X., Abreu, J. G., Yokota, C., MacDonald, B. T., Singh, S., Coburn, K. L., Cheong, S. M., Zhang, M. M., Ye, Q. Z., Hang, H. C., Steen, H., and He, X. (2012) Tiki1 is required for head formation via Wnt cleavage-oxidation and inactivation. *Cell* **149,** 1565–1577
9. Zhang, X., Cheong, S. M., Amado, N. G., Reis, A. H., MacDonald, B. T., Zebisch, M., Jones, E. Y., Abreu, J. G., and He, X. (2015) Notum is required for neural and head induction via Wnt deacylation, oxidation, and inactivation. *Dev. Cell* **32,** 719–730
10. Kakugawa, S., Langton, P. F., Zebisch, M., Howell, S. A., Chang, T. H., Liu, Y., Feizi, T., Bineva, G., O'Reilly, N., Snijders, A. P., Jones, E. Y., and Vincent, J. P. (2015) Notum deacylates Wnt proteins to suppress signalling activity. *Nature* **519,** 187–192
11. MacDonald, B. T., Hien, A., Zhang, X., Iranloye, O., Virshup, D. M., Waterman, M. L., and He, X. (2014) Disulfide bond requirements for active wnt ligands. *J. Biol. Chem.* **289,** 18122–18136
12. Dunny, G. M. (2013) Enterococcal sex pheromones: signaling, social behavior, and evolution. *Annu. Rev. Genet.* **47,** 457–482
13. Chandler, J. R., Flynn, A. R., Bryan, E. M., and Dunny, G. M. (2005) Specific control of endogenous cCF10 pheromone by a conserved domain of the pCF10-encoded regulatory protein PrgY in *Enterococcus faecalis*. *J. Bacteriol.* **187,** 4830–4843
14. Chandler, J. R., and Dunny, G. M. (2008) Characterization of the sequence specificity determinants required for processing and control of sex pheromone by the intramembrane protease Eep and the plasmid-encoded protein PrgY. *J. Bacteriol.* **190,** 1172–1183
15. Bazan, J. F., Macdonald, B. T., and He, X. (2013) The TIKI/TraB/PrgY family: a common protease fold for cell signaling from bacteria to metazoa? *Dev. Cell* **25,** 225–227
16. Sanchez-Pulido, L., and Ponting, C. P. (2013) Tiki, at the head of a new superfamily of enzymes. *Bioinformatics* **29,** 2371–2374
17. Gomis-Rüth, F. X. (2008) Structure and mechanism of metallocarboxypeptidases. *Crit. Rev. Biochem. Mol. Biol.* **43,** 319–345
18. Rawlings, N. D., and Barret, A. J. (2004) Introduction: metallopeptides and their clans. in *Handbook of Proteolytic Enzyme* (Barret, A. J., Rawlings, N. D., and Woessner, J. F., eds) 2nd Ed., pp. 231–268, Academic Press, San Diego
19. Mao, B., Wu, W., Davidson, G., Marhold, J., Li, M., Mechler, B. M., Delius, H., Hoppe, D., Stannek, P., Walter, C., Glinka, A., and Niehrs, C. (2002) Kremen proteins are Dickkopf receptors that regulate Wnt/β-catenin signalling. *Nature* **417,** 664–667
20. Meyer, B. S., and Rademann, J. (2012) Extra- and intracellular imaging of human matrix metalloprotease 11 (hMMP-11) with a cell-penetrating FRET substrate. *J. Biol. Chem.* **287,** 37857–37867
21. Morar, M., Pengelly, K., Koteva, K., and Wright, G. D. (2012) Mechanism and diversity of the erythromycin esterase family of enzymes. *Biochemistry* **51,** 1740–1751
22. Chandler, J. R., and Dunny, G. M. (2004) Enterococcal peptide sex pheromones: synthesis and control of biological activity. *Peptides* **25,** 1377–1388